CHAPTER 3

In this chapter, the methods, which were applied to the data are briefly introduced.

3. Methods

Two different methods were used in this thesis to study the lithospheric structure at the study area.

3.1 P-to-S receiver function method

The teleseismic P receiver function method has become a popular technique to constrain crustal and upper mantle velocity discontinuities under a seismic station (e.g. Langston, 1977; Owens et al., 1984; Kind and Vinnik, 1988; Ammon, 1991; Kosarev et al, 1999; Yuan et al., 2000). Telesismic body waveforms recorded at a three-component seismic station contain a wealth of information on the earthquake source, the earth structure in the vicinity of both source and the receiver, and mantle propagation effects. The resulting receiver function is obtained by removing the effects of source and mantle path.

The basic aspect of this method is that a few percent of the incident P wave energy from teleseismic events at significant and relatively sharp velocity discontinuities in the crust and upper mantle will be converted to S wave (Ps), and arrive at the station within the P wave coda directly after the direct P wave (Fig. 3.1). Ps converted waves are best observed at epicentral distances between 30° and 95° and are contained

largely on the horizontal components. The amplitude, arrival time, and polarity of the locally generated Ps phases are sensitive to the S-velocity structure beneath the recording station.

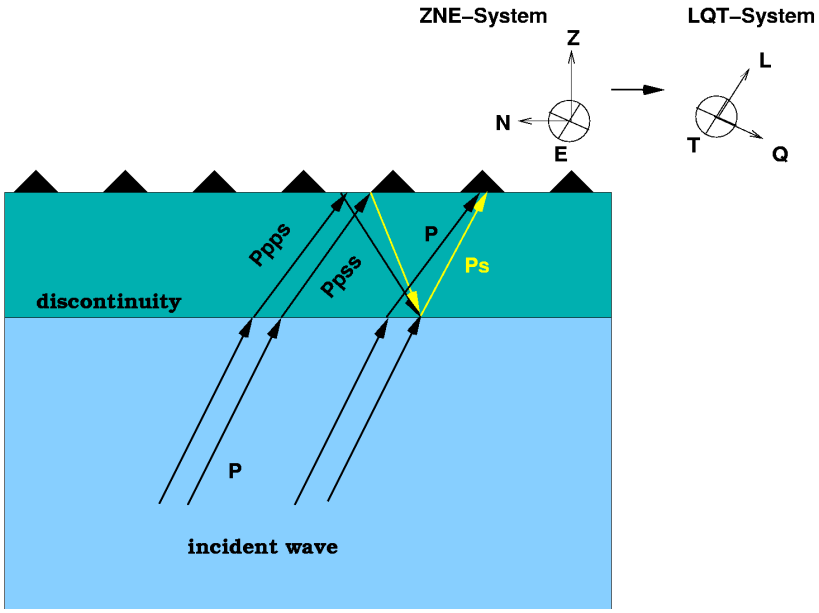

Fig. 3.1. Sketch illustrating P-S converted phase for an incident P wave from below on a homogeneous, isotropic layer with velocity V1>V2. Asides from primary Ps converted phase, two multiples (indicated by Ppss and Ppps) arriving later than Ps at the station are observed. To isolate the converted Ps wave from the direct P wave, the seismograms (ZNE) are rotated into an LQT ray-based system. The L component is in the direction of the incident P wave; the Q component is perpendicular to the L and the T component is the third component of the LQT right hand system.

By calculating the time difference in arrival of the converted Ps phase relative to the the direct P wave, the depth of the discontinuity can be estimated using a reference velocity model (in this thesis, the IASP91 reference velocity model is used). After rotating the coordinate system into a local LQT (P-SV-SH) recording system (Fig. 3.1), in which the L component is in the direction of the incident P wave, the Ps energy is mostly observed on the Q component perpendicular to the L component. The Q components (P receiver functions) contain Ps converted waves as well as related S type multiples. To obtain the P receiver function, the following steps are

generally used.

3.1.1 Restitution

Different seismographs are usually deployed to record earthquakes. Our data set(Table1, Appendix A), due to using several networks, consists of various instruments with quite different frequency responses.

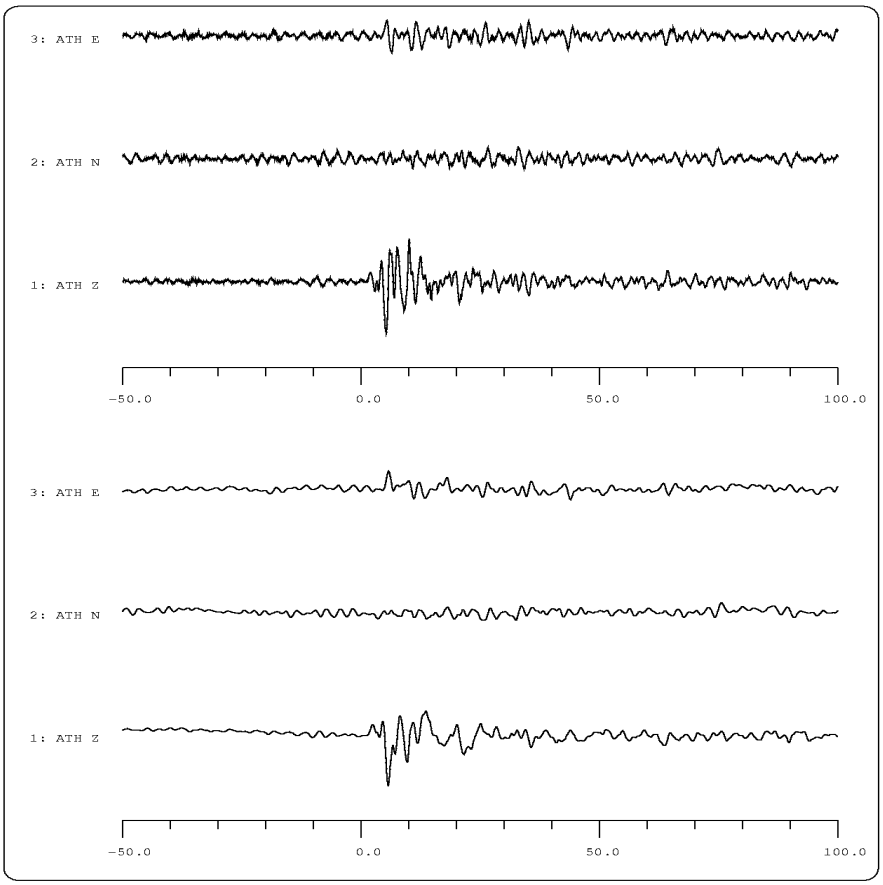

Fig. 3.2. Three components seismogram before and after restitution. The upper panel shows an original recording of the earthquake recorded at station ATH. Lower panel indicates the components after restitution of the instrument response. The P onset is assumed to be as zero time.

To utilize data recorded at different types of seismometers, the instrument responses have to be deconvolved. The main frequency range of teleseismic body waves is

between 1-0.1 Hz. Figure 3.2 shows an example of a three components record before and after restitution.

3.1.2 Rotation

Firstly, the two horizontal components N and E are rotated to radial (R) and tangential (T) directions. Most of the energy of the direct P and Ps waves are dominating the Z and R components, respectively. To isolate the converted Ps wave from the direct P wave, the ZRT components are rotated into an LQT (P-SV-SH) ray-based coordinate system, in which the L component is in the direction of the incident P wave; the Q component is perpendicular to the L component and is positive away from the source; the T component is the third component of the LQT right hand system. The L component is dominated by the P wave, while the Q and T components contain mainly the converted S wave energy (Fig. 3.3). For horizontally layered homogeneous media, the converted S wave energy is exclusively contained in the Q component. Presence of significant energy in the T component indicates dipping and/or anisotropic structure.

However, a correct estimation of the incidence angle of arriving P wave is the main requirement to perform a perfect rotation. Overestimation or underestimation of the incidence angle can result in some P wave energy on the Q component of the receiver functions at the time of direct P wave (P-onset). Fortunately, these uncertainties only affect the observed delay times of the P-to-S conversions from very shallow conversions (the first 1-2 s).

The azimuth and incidence angle of incoming P waves can be either theoretically calculated or actually measured. Theoretical back azimuth and incidence angle are calculated from the locations of the recording station and the earthquake hypocenter, and are usually used in the case of low signal-to-noise P wave signals.

If the incidence angle and azimuth of the incoming P wave are correctly estimated and the conversion phases do not originate from discontinuities dipping more than 10° (Langston, 1977), the isolating of the SV energy in the P coda is achieved and there

will be no P wave energy left on the Q and T components. Moreover, since the first onset on the Q component is the converted Ps phase from a shallow discontinuity below the surface, it is theoretically possible to detect discontinuities even at shallower depth (sediment layer) in contrast to the radial component where the direct P arrival usually covers Ps conversions from very shallow reflectors. Figure 3.3 indicates the rotated seismograms of the event shown in Figure 3.2.

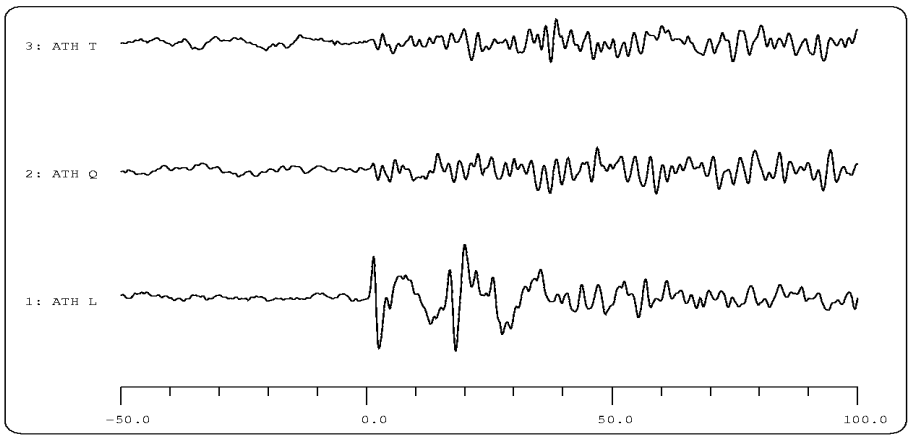

Fig. 3.3. Three components record shown in Figure 3.2 after rotation into LQT ray-based system. P waves and converted S waves dominate the L and Q components, respectively. The T component shows information about dipping or/and anisotropy.

3.1.3 Deconvolution

To eliminate the influence of the source and ray path, an equalization procedure is applied by deconvolving the Q and T component seismograms with the P signal on the L component (Yuan et al., 2000, 2002).

The resulting Q component data are named P receiver functions and are mainly composed of the P-to-S converted energy and contain information on the structure beneath a seismic station (Fig. 3.4). The arrival time of the converted Ps phase in receiver functions depends on depth of the discontinuity, whereas the amplitude of the converted phase depends on the S-wave velocity contrast across the discontinuity.

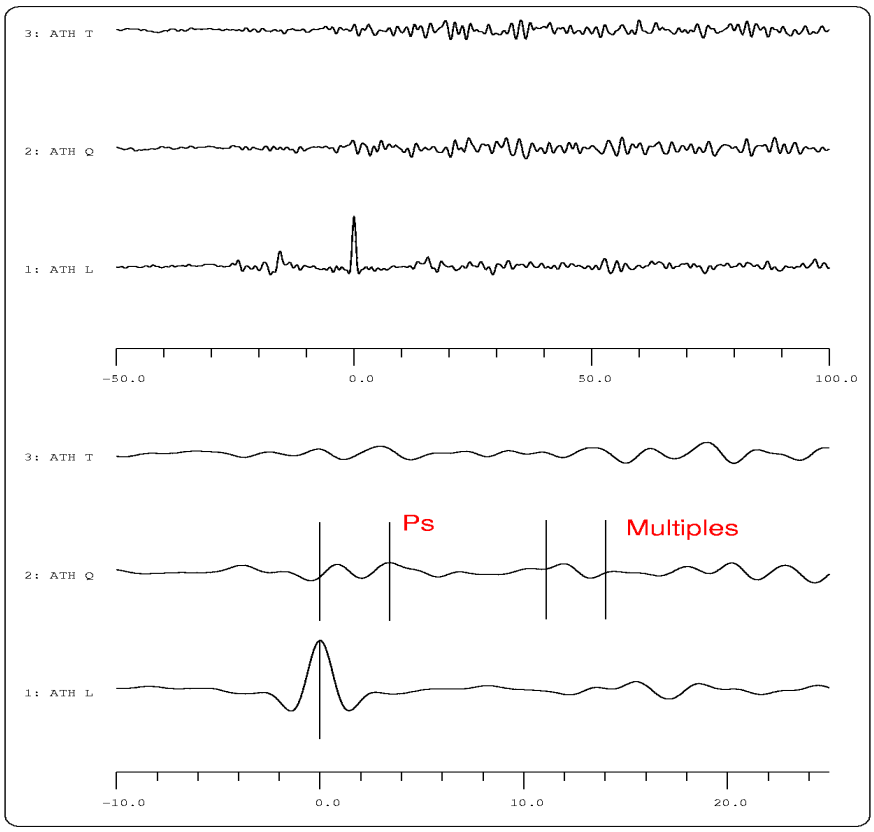

Fig. 3.4. P waveform is deconvolved from all three components. The L component indicates a spike waveform and the most converted Ps energy is contained on the Q component called P receiver function. The P onset is shifted to be as zero time. The three components are shown in the lower panel in the time window of -10-25 s. The first converted Ps phase at 3.5s represents the conversion from the Moho, while the multiples arrive at 11-14s delay time.

The final P receiver function contains, aside from the primary converted phases, multiple phases generated by each velocity discontinuity and reflected between the earth's surface and these discontinuities (Fig. 3.5). As an example, Figure 3.5 shows a simple isotropic and homogeneous model with one discontinuity at 30 km. Vs and depth values are represented in the upper panel.

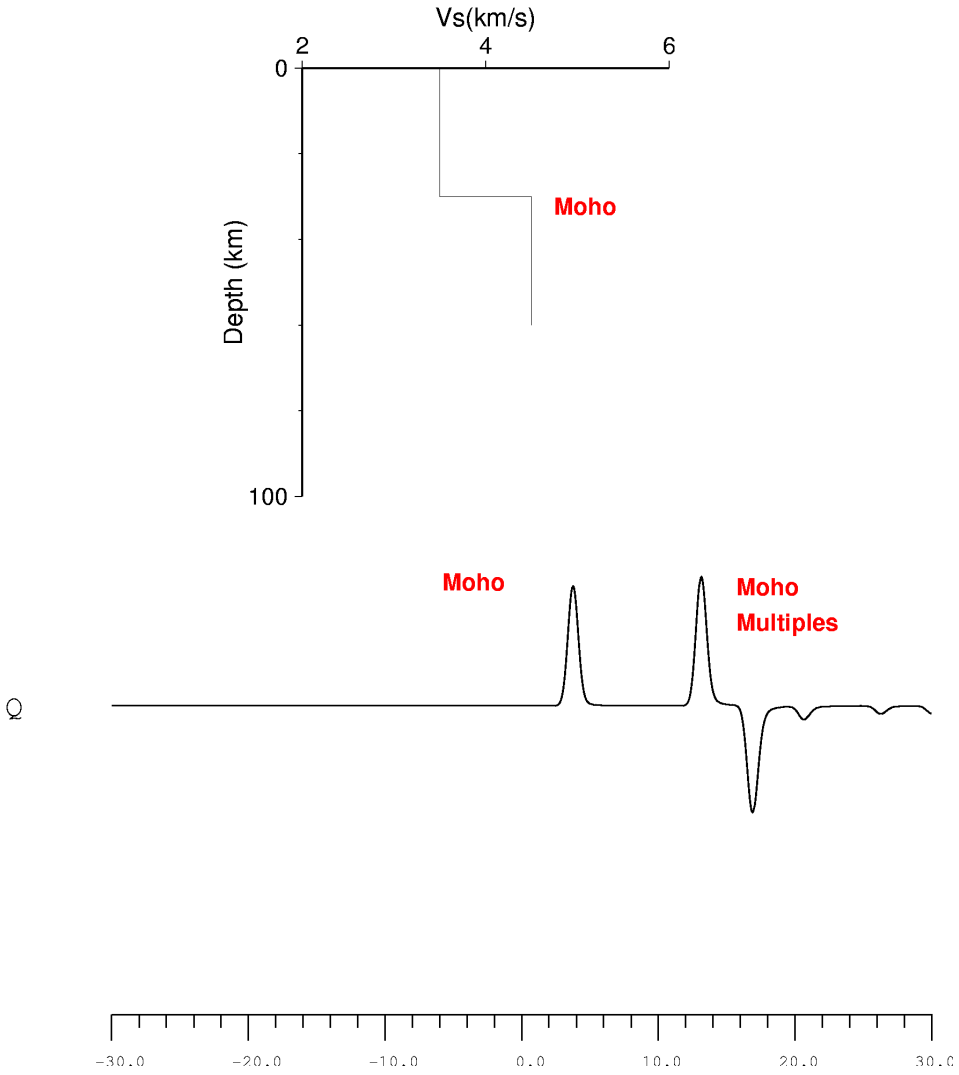

Fig. 3.5. Synthetic P receiver function produced for a layer over a half space shown in the upper panel. The Moho discontinuity lies at 30 km. The P receiver function reveals a very strong phase with positive amplitude at 3.5 s which is the converted Ps phase at the Moho. The multiples arrive at 13 s and 16 s delay time and show the Ppss and Ppps reverberations between earth's surface and the Moho.

The obtained synthetic P receiver function shows three strong phases; the first phase is the converted Ps phase from the Moho boundary at 30 km, which arrives at about 3.5 s; two other phases indicate multiples which reverberate between earth's surface and discontinuity and arrive at about 13 and 16 s delay time, respectively. Positive amplitudes in the receiver function reveal a velocity increase with depth, while

negative amplitudes indicate a velocity decrease with depth. Including multiples paths in the receiver function analysis (it they are properly identified) gives additional information about the exact depth of the Moho discontinuity and the crustal Poisson's ratio (Zandt et al., 1995; Zhu and Kanamori, 2000; Yuan et al., 2002). However, the presence of significant sediments may alter the primary Ps converted phases and make the estimation of the discontinuity depth difficult. An other problem occurs if a dipping interface changes the ray geometry or an anisotropic layer causes shear wave splitting effects. In both cases converted energy is expected to be observed on the T components. However, the major structure can be detected by analyzing the Q components. The energy on the transverse components gives additional information on the crustal heterogeneity or anisotropy (Cassidy, 1992; Levin and Park, 1997).

3.1.4 Moveout correction (distance equalization)

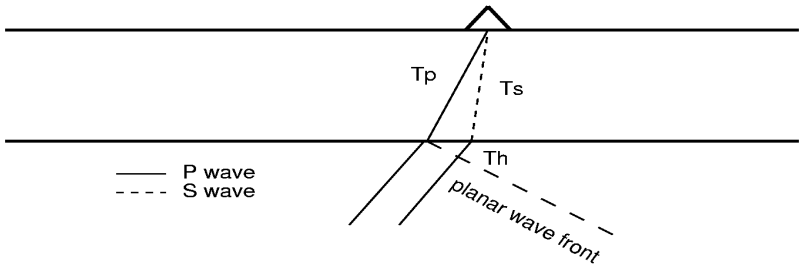

Fig. 3.6. Scheme showing the ray paths of direct P wave and converted Ps wave for a layer over a half space. Tp and Ts indicate the arrival times of P and S waves, respectively. The same ray parameter is assumed for both phases.

The converted Ps phases are usually weak and of low amplitude. In order to increase signal-to-noise, it is necessary to align and stack receiver functions from different epicentral distances at each station. However, successful alignment and constructive summation of conversion phases requires that the receiver functions be equalized in terms of their ray parameters.

For simplicity, a single layer over a half space is considered in Fig. 3.6. The ray paths

of the incident P and the converted Ps phases are also shown. Regarding to epicentral distances (>30 °), it is acceptable to approximate the incoming P waves as plane waves and accordingly formulate the Ps-P delay time as:

$$Tps - Tp = Ts + Th - Tp \qquad (3.1)$$

Assuming that the ray parameter is the same for P and Ps it can be shown (Kind & Vinnik, 1988) that,

$$Tps - Tp = h((Vs^{-2} - p^2)^{1/2} - (Vp^{-2} - p^2)^{1/2} \qquad (3.2)$$

and following the same line of argument the delay times for important crustal reverberations (multiples) are calculated as follow:

$$TPpPs - Tp = h((Vs^{-2} - p^2)^{1/2} + (Vp^{-2} - p^2)^{1/2} \qquad (3.3)$$

$$TPpSs/PsPs = 2h(Vs^{-2} - p^2)^{1/2} \qquad (3.4)$$

$$TPsSs = h(3(Vs^{-2} - p^2)^{1/2} + (Vp^{-2} - p^2)^{1/2} \qquad (3.5)$$

The conversion from crust-mantle boundary, its crustal multiples and the upper mantle 410 km and 660 km discontinuities arrive at the recording station with different slowness values (Fig. 3.7).

An approach similar to familiar normal move-out correction in exploration seismology, is taken to adjust the times of Ps conversions of all receiver functions with respect to the arrival time of the Ps conversion at a reference epicentral distance of 67° (corresponding to ray parameter of 6.4 sec/°) according to a global one dimensional velocity model (IASP91 reference velocity model).

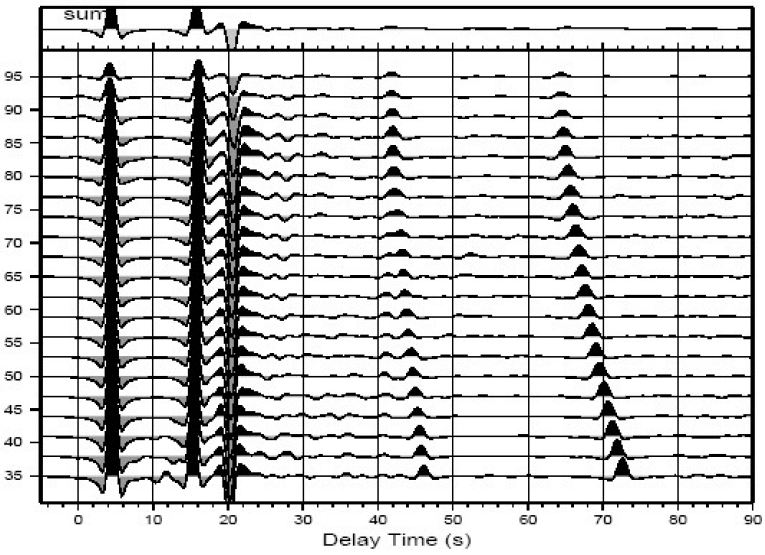

Fig. 3.7. Synthetic P receiver functions at a single station are computed using the reflectivity method. The IASP91 model is modified to contain a 40 km thick crust. Crustal Vp and Vs are assumed to be 6.5 and 3.75 km/s, respectively. Epicentral distances range between 35-95° and the focal depth is fixed at 600 km. By increasing epicentral distance, the delay times of Ps conversion decrease, while those of the multiples increase.

After correction, all direct conversions from Moho and upper mantle appear as straight lines, whereas crustal multiples become more inclined (Fig. 3.8). Stacking the moveout corrected receiver functions (for Ps) enhances the direct conversions, while the multiples are considerably weakend.

Move-out correction, as described before, can also be applied to crustal multiples. Applying the correction to each multiple and aligning the corrected seismograms by epicentral distance leads to straight appearance of the multiples whereas the direct conversions are more inclined. In this case, after correction, the multiples which have similar ray parameters appear parallel to each other.

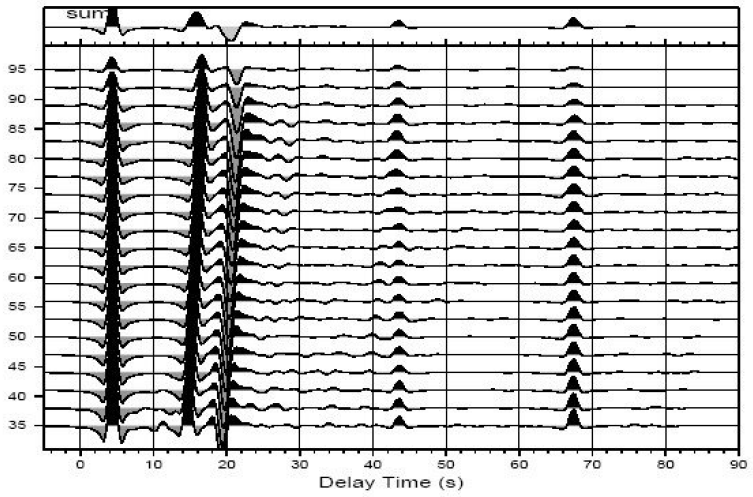

Fig.3.8. Ps moveout corrections for P receiver functions shown in Fig. 3.7. Move-out time corrections for Ps waves are applied to each sample in the receiver functions. IASP91 reference model and reference slowness of 6.4 s/ ° are used. Ps converted phases of Moho and upper mantle discontinuities at 410 and 660 km are aligned vertically, while the multiples are inclined. The summation trace in the upper panel shows the enhanced amplitudes of the primary converted phases and weakend amplitudes for multiples.

3.1.5 Migration

To improve the spatial resolution and convert the delay times into depths, the Ps amplitudes on each receiver function can be back projected along the ray path onto the spatial locations of the conversion points to their true locations in a process similar to migrating in exploration seismology (Kosarev et al., 1999)(Fig. 3.9). The ray paths are calculated using a one dimensional global velocity model (IASP91) with assumption that conversions are produced from planar interfaces. Sometimes a spatial smoothing filter is used to improve the spatial correlation so that the space is gridded and back projected amplitudes originating from adjacent boxes are stacked to improve signal to noise ratio.

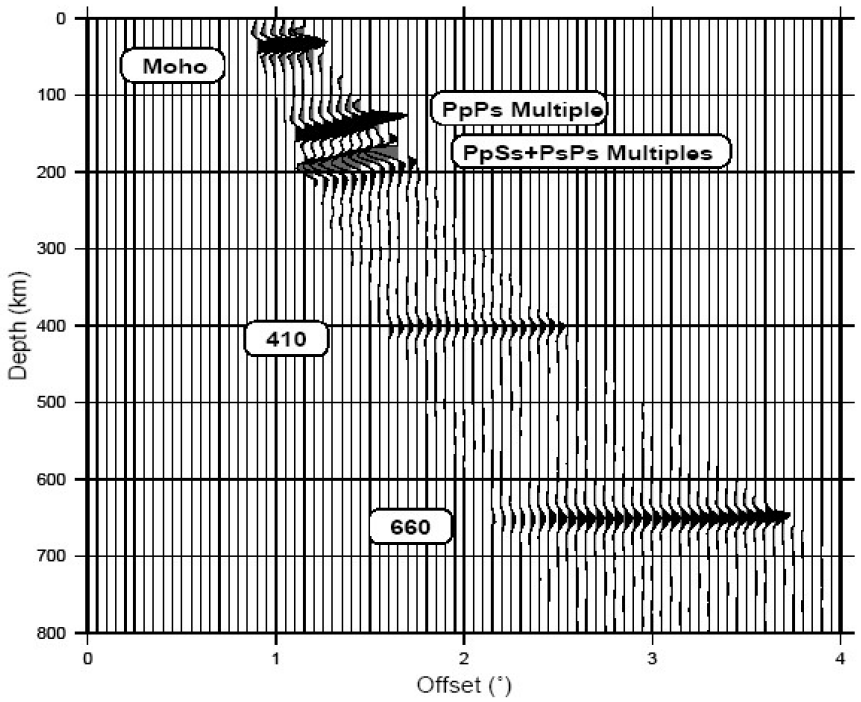

Fig.3.9. Migrated receiver functions of synthetic traces shown in Figure 3.7. Ps conversions are back-projected to horizontal images. The phases are labeled. The straight appearance of direct converted phases helps to distinguish them from oblique crustal multiples.

Applying the method to data from stations and networks where ray paths from neighboring stations, specially at large depths cross one another, improves the signal quality significantly. Besides, projection of 3-D data along desired 2-D sections can further amplify the conversion amplitudes while suppressing the reverberations due to their oblique appearance (Fig. 3.9). The technique can also be applied to reverberations of conversions and thus provide an additional possibility for detecting direct conversions.

3.1.6 Estimation of crustal thickness and Vp/Vs ratio

The converted Ps phase and crustal multiples (PpPs, PpSs and PsPs) contain a wealth of information concerning the average crustal properties such as the Moho depth and the Vp/Vs ratio.

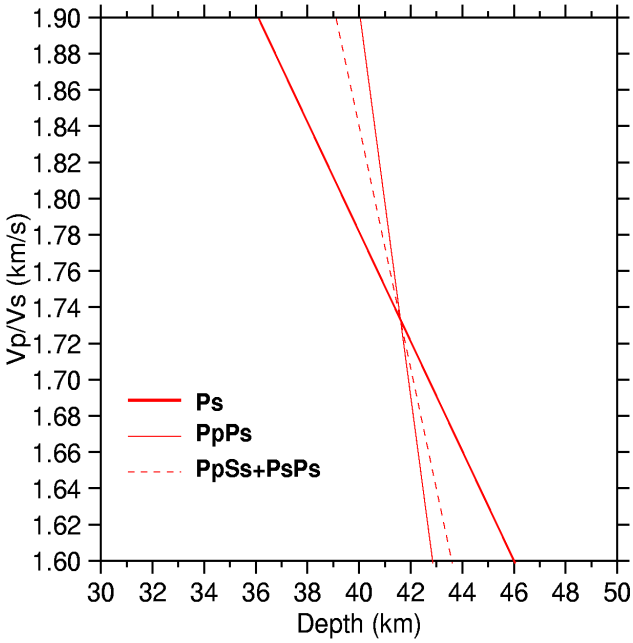

Fig. 3.10. Contributions of Ps and its multiples to the stacked amplitude as a function of crustal thickness (h) and Vp/Vs ratio.

The delay times of the primary converted Ps phase from the Moho and its crustal multiples can be used to determine the crustal thickness by a given average crustal P velocity. In presence of clear multiples, the Moho depth and Vp/Vs ratio can be computed using the stacking method of Zhu and Kanamori (2000).

This algorithm stacks the amplitudes of receiver functions at the predicted arrival time of the Moho conversion (Ps) and its multiples (PpPs and PpSs+PsPs) for various crustal thicknesses h and Vp/Vs ratios. The time domain receiver functions are then plotted by means of crustal thickness versus Vp/Vs ratio (Fig. 3.10). Regarding the higher signal to noise ratio of the primary converted phase (Ps) in comparison to its multiples, amplitudes of phases are weighted and stacked as following:

$$S(h,Vp,Vs) = w1Q(t1) + w2Q(t2) - w3Q(t3) \quad (3.6)$$

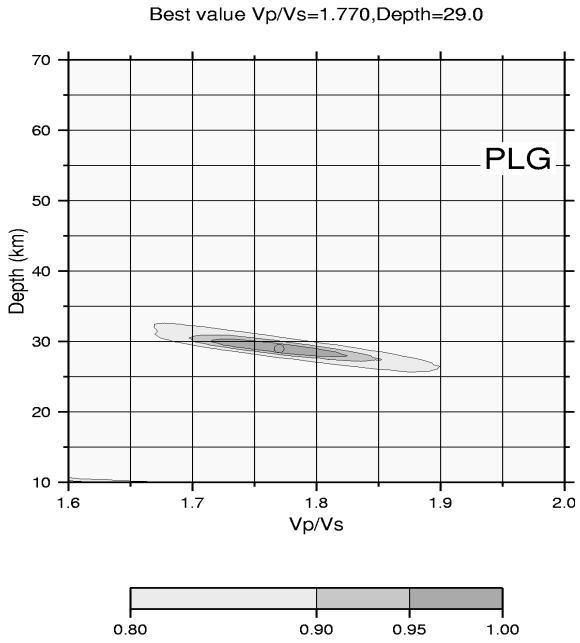

Fig. 3.11. Applying Zhu and Kanamori method for station PLG. The amplitude is shown in the lower part and ranges from 0.8 to 1. The optimal combination of the crustal thickness and Vp/Vs ratio is defined where the largest amplitude (1) occurs. The circle shows a Moho depth of 29 km and Vp/Vs of 1.77 for this station.

where Q(ti) are the receiver function amplitudes, t1, t2 and t3 are the predicted travel times for Ps, PpPs and PpSs+PsPs corresponding to crustal thickness h and Vp/Vs ratio and w shows the weighting factor for each phase. The highest weighting factor is associated with the direct conversion (w1>w2+w3), as the slopes of crustal multiples are very similar. The function S(h,Vp,Vs) reaches a maximum when all three phases (Ps,PpPs and PpSs+PsPs) are stacked coherently. The obtained h (crustal thickness) and Vp/Vs ratio are also considered as the best combination underneath the assumed station if the multiples are clear enough. As an example, Fig. 3.11 indicates the computed crustal thickness and Vp/Vs ratio for station PLG.

3.2 S-to-P receiver function method

Although P-to-S receiver function analysis has become a routine method to detect the Moho and upper mantle discontinuities underneath a seismic station, S-to-P receiver function technique is still not developed.

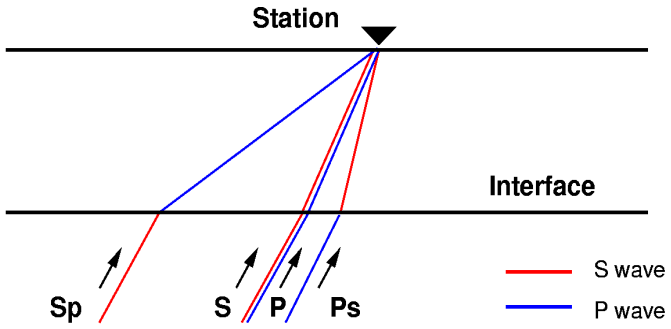

Fig. 3.12. Ray paths of Sp and Ps converted phases.

The P receiver function technique looks for the P-to-S conversions at seismic discontinuities beneath stations, while S receiver function analysis searches for the S-to-P conversions at the seismic discontinuities.

A Sp phase is generated when an incoming S phase crosses a velocity discontinuity beneath a seismic station and is converted to the P wave (Fig. 3.12). For a particular station, the converted Sp phase arrives earlier than the direct S phase (e.g. Faber and Müller, 1980; Bock, 1991; Farra and Vinnik, 2000; Li et al., 2004 ; Kumar et al., 2005). Converted Sp phases from shallow discontinuities (like crust-mantle and lithosphere-asthenosphere boundaries) are best observed at epicentral distances between 60-85° (Faber and Müller, 1980). In the case of larger distances (larger than 85°), SKS phases arrive earlier than S waves and these converted phases have to be considered.

The method used to compute P receiver functions can be also performed for S receiver functions. This method includes coordinate rotation and deconvolution. Similar to the P receiver function technique, the Q component is perpendicular to the L component, which is located in the direction of the incident S wave. It is positive away from the source. The sign of the receiver function amplitude is also related to the velocity contrast. Positive amplitudes show velocity contrasts with velocity increasing downwards, while negative amplitudes showing that the velocity decreases with depth. S receiver functions are much noisier than P receiver functions primarily because they arrive after the P wave. They also have longer periods in comparison with the P receiver functions and do not resolve the fine structure within the crust and mantle lithosphere. However, they are precursors to S waves, whereas all the multiple reverberations appear later than S. This advantage, that they are free of multiples enables them to separate the primary converted phases from the disturbing multiples, which are not more visible. The boundaries, which are normally covered by multiples arriving at nearly the same time in the P receiver functions, can also be identified in the S receiver functions.

Fig. 3.13 demonstrates a simple two layered model over a half space containing crust-mantle and lithosphere-asthenosphere boundaries at about 30 and 125 km, respectively. The synthetic P and S receiver functions are computed and compared. The P onset (for P receiver function) and S onset (for S receiver function) are fixed to be on zero. While Ps converted phase arrives later than direct P phase, the converted Sp phase is precursor of direct S wave and arrives earlier. As Figure 3.13 shows, all multiples arrive after direct S wave, therefore they can not disturb the major conversions. The computed P receiver function shows the converted Ps phase at Moho as well as its multiples. The converted phase from lithosphere-asthenophere boundary is covered by the multiples arriving at the same time on the P receiver function, even though this boundary is significantly observed on the S receiver function at 13 s (reversed time). Assuming the same ray parameter, the arrival time of the converted Sp phase at Moho is similar to that of P receiver function but in the reversed time (3.5 s). Different sign of the S-to-P conversion coefficients relative to those of P-to-S

conversion makes a reversed polarity for Sp converted phase.

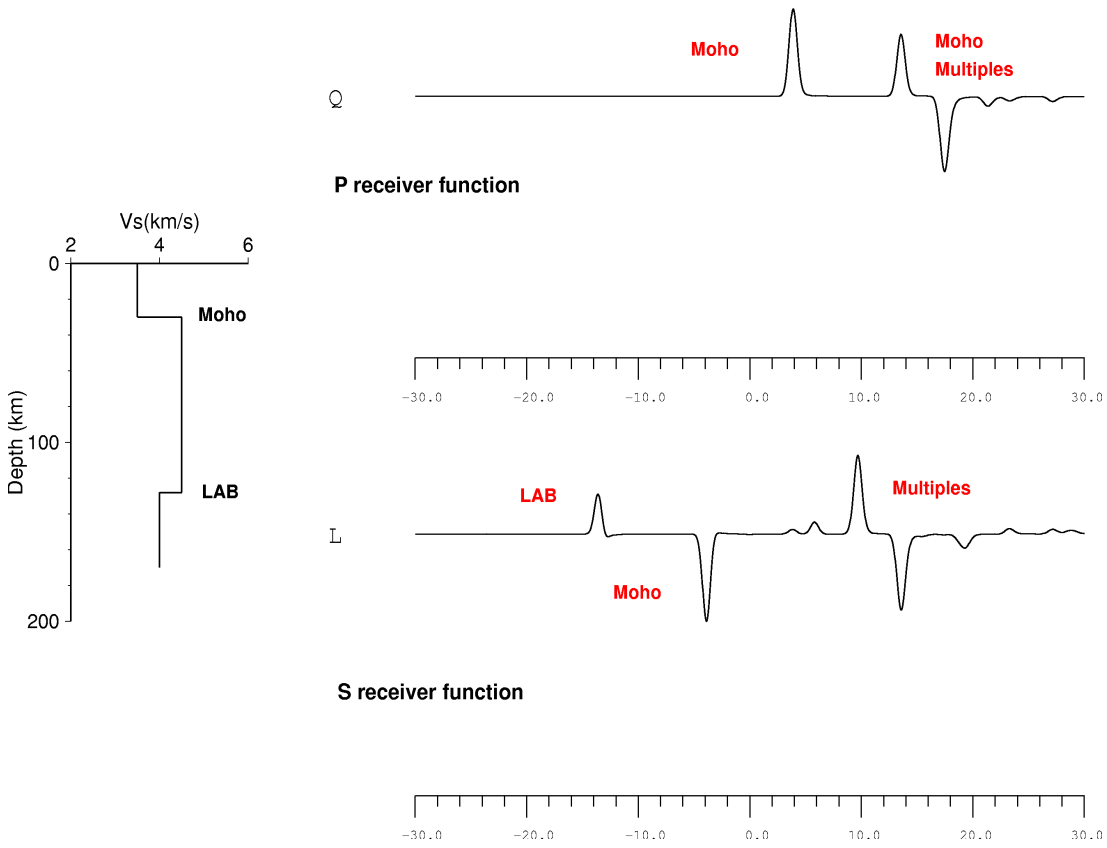

Fig. 3.13. Synthetic P and S receiver functions are computed for a two layered model over a half space shown in left part of the Figure. Two discontinuities are defined in the model as crust-mantle and lithosphere-asthenophere boundaries at 30 and 125 km, respectively. The S velocities are considered to be 3.5 km/s in the crust and 4.5 s in the upper most mantle. The P onset for P receiver function as well as S onset for S receiver function are fixed to be as zero time. P receiver function significantly reveals the Ps conversion and its multiple phases from the Moho, while the lithosphere-asthenosphere boundary (labeled with LAB) is masked by the crustal multiples. In contrast, S receiver function reliably shows the Sp converted phase from the Moho as well as that from the LAB. Sp phases arrive earlier than direct S waves, whereas all the multiples appear later. With this advantage the S receiver function separates the primary converted phases from disturbing multiples. The polarity of the Sp converted phase is reversed due to the different sign of its conversion coefficient comparing to that of Ps.

3.2.1 Lithphosere-asthenosphere boundary

The Earth's tectonic plates constitute the lithosphere so no proper understanding of plate tectonics can be achieved without reference to the lithosphere, and this requires an understanding of its essential difference from the asthenosphere. The lithosphere is generally divided into two different parts. The crust lithosphere includes the upper part of the lithosphere, whereas the mantle lithosphere located in the lower part moves as the high velocity lid on the top of the asthenosphere. High viscosity lithospheric plates moving over a lower viscosity asthenosphere is one of the basic aspects in studying plate tectonics. Observations of low seismic velocities in the upper mantle are generally associated with the lithosphere-asthenosphere boundary named LAB. This boundary appears as a negative contrast in which the seismic velocities decrease with depth. In contrast to the Moho depth which is usually observed at high resolution by different techniques such as P receiver function method, the lower boundary of the mantle lithosphere is generally considered not sharp enough to be well observed by seismic body wave observations. The thickness of the lithosphere has been mostly obtained from low resolution surface wave observations. The lithosphere has a global average thickness of 80-100 km, ranging between zero and 200 km beneath mid ocean ridges and stable cratons, respectively. However, the recently developed S receiver function technique (Li et al., 2004; Kumar et al., 2005) can be optimally used to identify the LAB boundary using higher resolution body waves, since this method is free of multiples. This boundary is almost invisible in the P receiver functions due to the crustal multiples, which arrive at the same time and heavily disturb the time window of the LAB arrival.

3.2.2 Processing

The new S receiver function technique complements the well known S-to-P receiver function method and adds only some new steps in its processing. The first step to

apply the S receiver function method is to collect the suitable events with magnitude larger than 5.7 and epicentral distances between 60-85°, which show a clear S wave. Figure 3.14 shows an event recorded at a three components broadband station. The arrival time of S wave can be clearly identified on the horizontal components (N,E). The seismograms can be also restituted, like in P receiver function technique, to have the same frequency response.

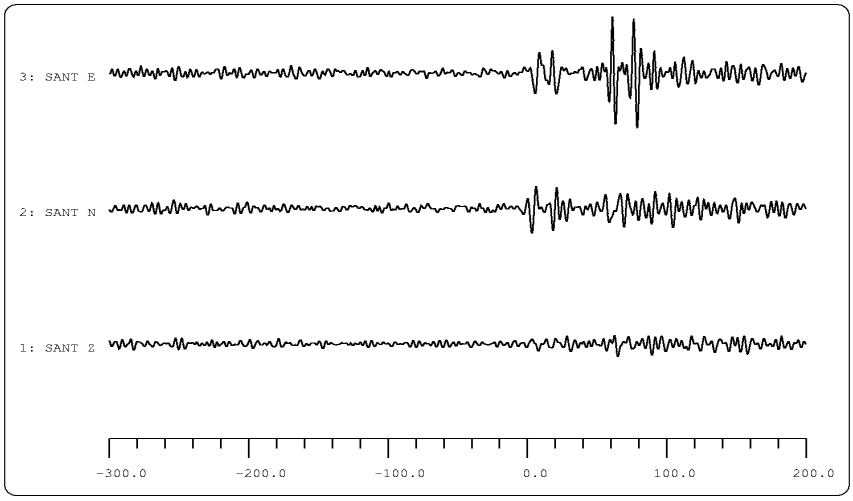

Fig. 3.14. Restituted three components seismogram shows a clear S arrival time on the horizontal components. The S onset time is shifted to be on zero.

3.2.3 Rotation

Similar to P receiver function method, the two horizontal components (N,E) are firstly rotated around the theoretical back azimuth to the radial and tangential directions (R,T). In the next step, the components are rotated into the LQT (P-SV-SH) system, as described in P receiver function method. However, rotation around the incidence angle in S receiver functions is even more important than in P receiver functions. A very accurate procedure has to be performed to choose the correct incidence angle. For this aim, a subroutine was used, which rotates components with a series of incidence angles.

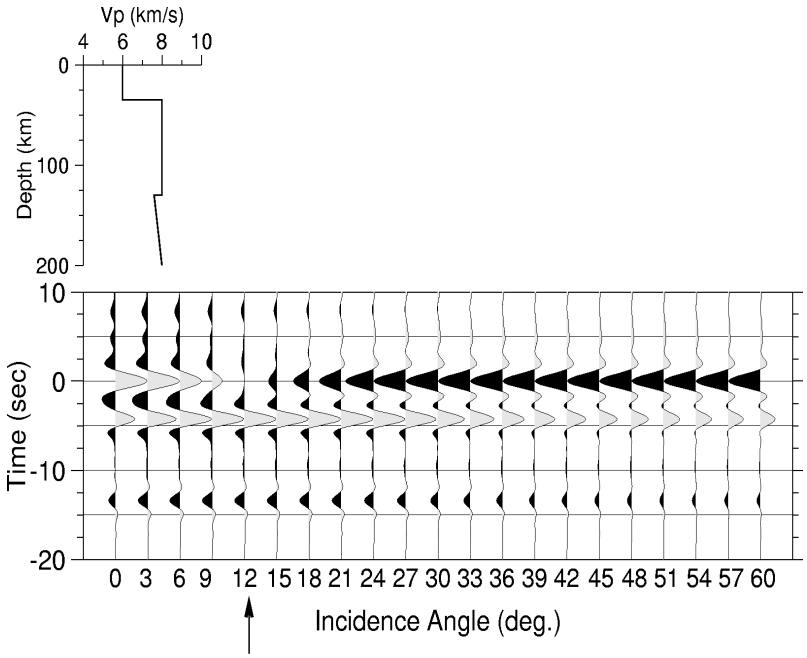

Fig.3.15. Determination of the incidence angle for synthetic seismograms for the shown model by rotating the vertical and radial components around the incidence angle. The synthetic seismograms are computed using reflectivity method for a simple model shown at the top. S receiver functions have been computed using different incident angles ranging between 0-60°. The theoretical incidence angle agrees well with the observed one (shown with arrow). The amplitude at the S arrival time (zero time) changes sign at that angle.

The method aims at having the least energy on the L (P) components at the time of S arrivals (S-onset). Figure 3.15 shows a simple model consisting of two discontinuities, a positive contrast at 30 km (Moho) and a negative contrast at 130 km (LAB). The synthetic seismograms have been generated using the reflectivity method (Kind, 1985) and the S receiver functions have been computed using different angles of incidence ranging between 0-60°. The lower panel shows the L (P) components obtained from various rotations. The deconvolution has also been applied to the L components (described in the next part). As the figure shows, the amplitude at the S arrival time (zero time) changes sign. The best incidence angle is chosen, where the minimum energy is observed on the zero time.

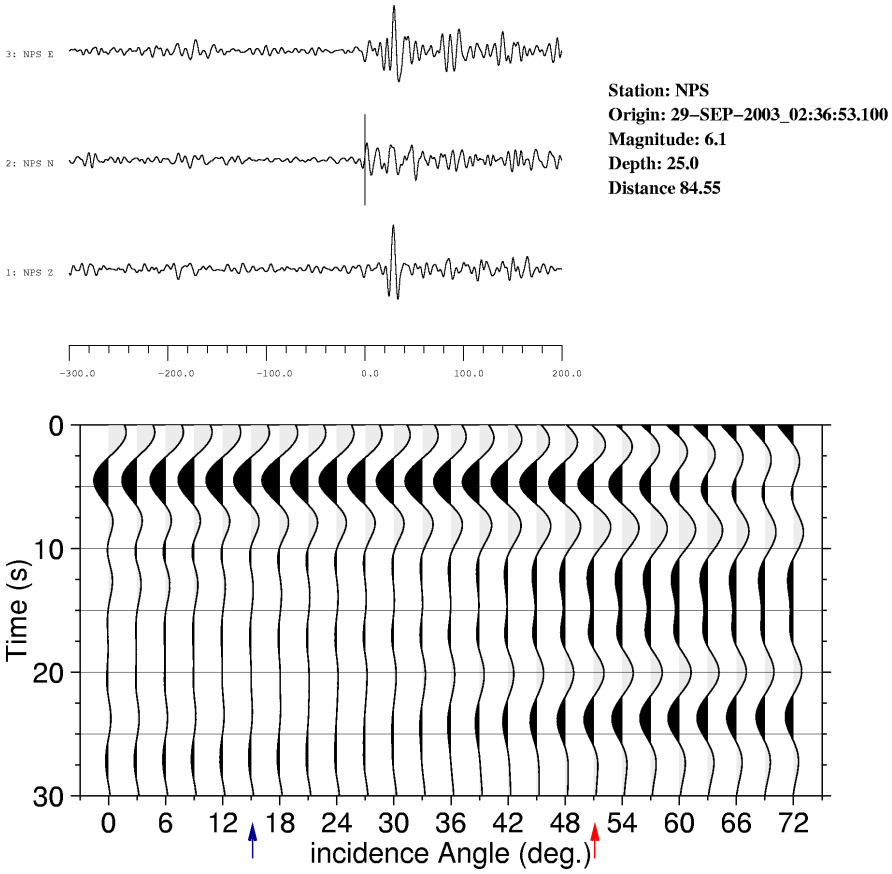

Fig.3.16. The L component has been rotated around different incidence angles ranging between 0-72°. The three components of the short period station as well as the event parameters are shown at the top of the Figure. The theoretical and observed incidence angles are indicated with blue and red arrows, respectively. The best incidence angle is defined where no energy on zero time occurs (51°), while the theoretical angle is at 15°.

For such a simple model, the theoretical incidence angle agrees well with the observed one (marked with arrow at 12°). However, in contrast to the P receiver function method, the selected incidence angle has a significant role in detecting the other major Sp converted phases. Taking an incorrect angle of incidence can enhance a noise phase and weaken a major converted phase in the whole seismogram. While in the P receiver function method, only the first 1-2 s of the seismogram will be affected by an incorrect incidence angle (shallow deep discontinuity).

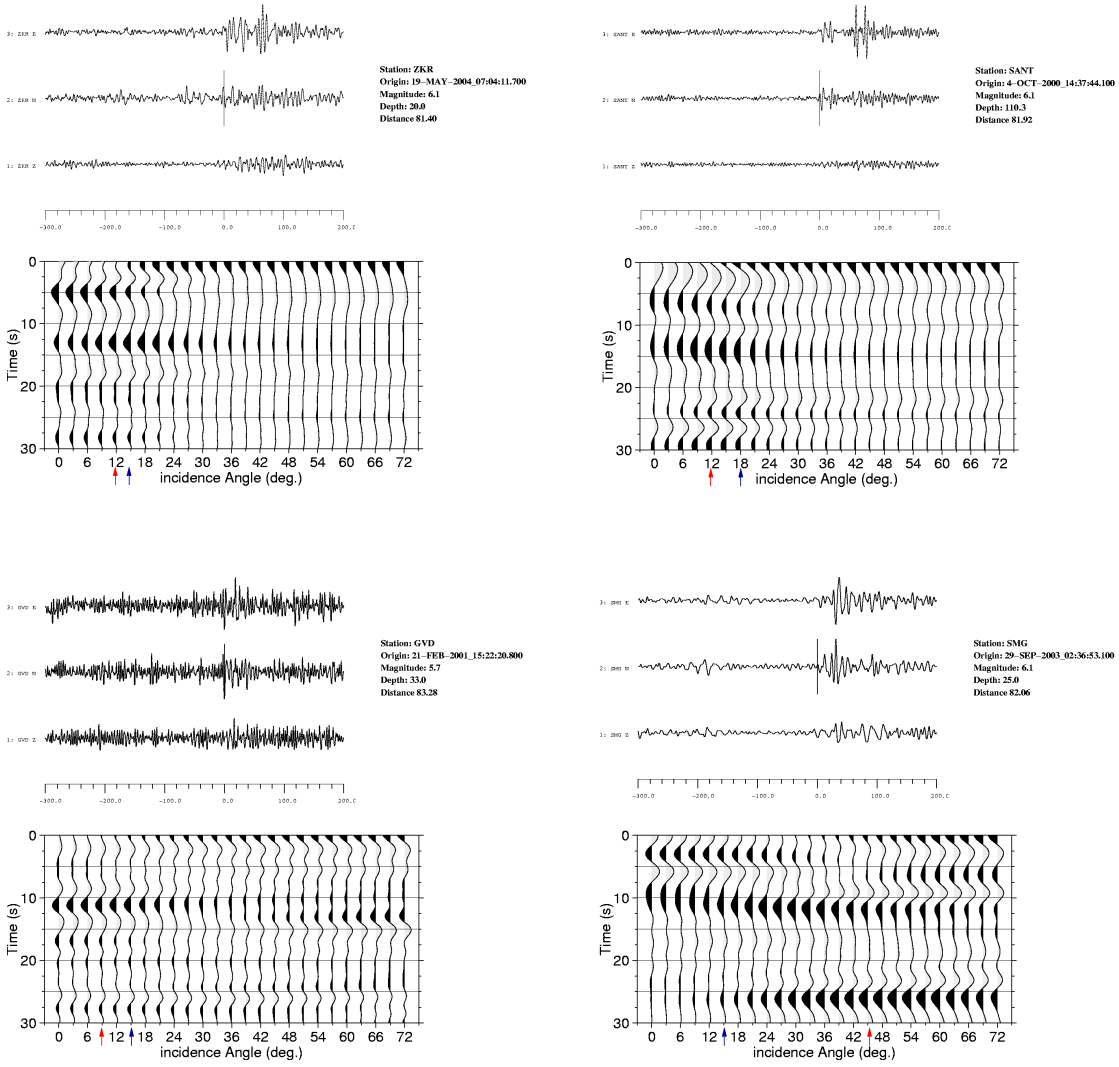

Fig.3.17. Some examples of rotation procedure used to estimate the best incidence angle. The blue and red arrows show the theoretical and observed incidence angle, respectively. This procedure results in a minimum P energy on the zero time and strong appearance of the major Sp converted phases in the whole seismogram.

Some examples shown in Figures 3.16-3.17 display the application of the rotation subroutine for different events. Figure 3.16 represents an event at 85° distance with magnitude of 6.1 recorded at short period station NPS. The S wave is quite sharp on the horizontal components. The S-onset arrival time is shifted to be as zero time. The lower panel shows the L components obtained from rotation around incidence angles of 0-72°. While the theoretical angle at 15° leaves some energy on zero time, a greater incidence angle at 51° shows the least energy on zero time and additionally enhances

the amplitude of the LAB converted phase at about 13 s. Therefore, a perfect rotation will be achieved if asides from the minimum energy on S-onset time, the major conversions are also well displayed on the L component.

3.2.4 Deconvolution

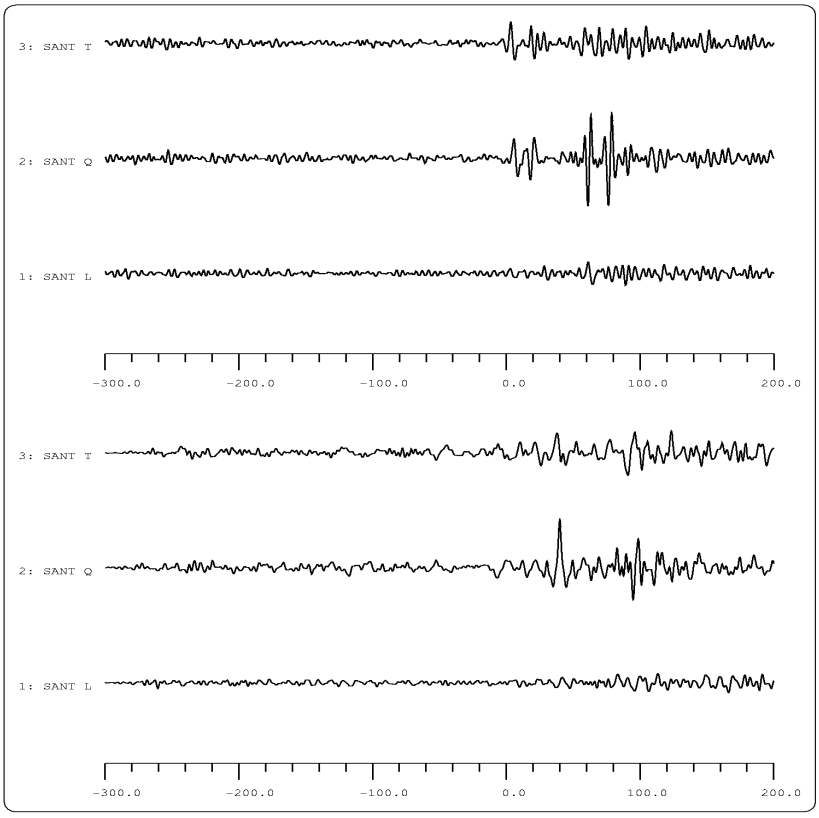

Fig. 3.18. The three components record shown in Figure 3.14 after rotation and deconvolution. The upper panel shows the rotated components around the theoretical back azimuth and observed incidence angle. In the lower panel all components are deconvolved with the S signal on the Q component. The most Sp energy dominates the L component.

After rotation, the converting Sp phases mostly dominate the L (P) components. In order to remove the S signal from the L components, the L components are deconvolved with the S signal on the Q components. The resulting L component, which contains only converted Sp phases (no multiples) is named S receiver function.

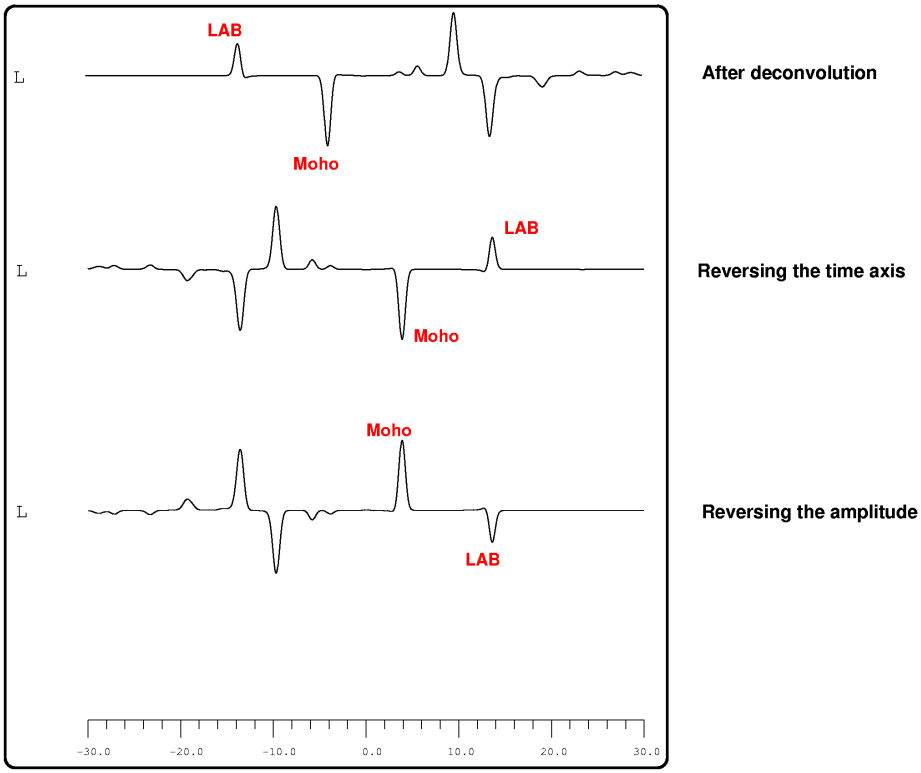

Fig. 3.19. Synthetic S receiver function after deconvolution has a reversed form comparing with the P receiver function. To compare it directly with P receiver function, the time axis as well as the amplitudes are reversed.

Figure 3.18 shows the seismograms indicated in Figure 3.14 after rotation and deconvolution. However, the coefficients of the S-to-P conversions have different signs than those of the P-to-S conversions. Figure 3.19 represents the computed S receiver function for the model shown in Figure 3.13. To make the S receiver function look like conventional P receiver function, some changes are needed. As Figure 3.19 shows, the resulted S receiver function has a reversed time axis compared to the P receiver function time axis. Therefore the time axis of the S receiver function has to be reversed in the first step. The different sign of the S-to-P conversion coefficients results in the reversed polarity of the S receiver function amplitudes. To remove this effect, the polarity of the S receiver function also has to be reversed. Finally, the resulted S receiver function can be directly compared with the P receiver function.

3.2.5 Moveout correction and stacking

The dependence of the arrival time of the Sp converted waves on the S wave slowness (move-out) has to be corrected for by using a reference slowness and a reference earth's model (like P receiver function). To directly compare the Sp and Ps receiver functions, the same reference slowness of 6.4 s/° (corresponding to epicentral distance of 67°) is also applied to S receiver functions, although this value is not realistic for S waves. Figure 3.20 shows the computed synthetic S receiver functions using the reflectivity method for a single station.

The IASP91 model is modified to contain the crust and lithosphere at 35 and 120 km, respectively. The P velocity is assumed to be 6.20 km/s in the crust and 8.0 km/s in the uppermost part of the upper mantle, which is reduced 5% at the lithosphere-athenosphere boundary. The S receiver functions of different events have been sorted according to their epicentral distances ranging between 60-110°. As Figure 3.20a shows, the variations of moveout curves get stronger with increasing conversion depth. For a shallow depth (Moho) the variation is very small, while delay time variations at LAB and upper mantle discontinuities become significantly larger. However, using a movout correction for Sp according to the reference slowness of 6.4 s/° helps to enhance the major Sp converted phases. Figure 3.20b indicates the S receiver functions after moveout correction. Moveout time corrections for Sp waves (reference slowness 6.4 s/°) are used for each sample in S receiver functions. After moveout correction, the converted Sp phases from the major discontinuities like Moho and LAB are aligned vertically, while the upper mantle discontinuities are not well aligned and have slightly oblique appearances. Since Sp conversion phases are usually weak signals, a number of records must be summed to obtain a good signal-to-noise ratio. The sum trace of the moveout corrected S receiver functions presents strong direct conversions from all major discontinuities, as shown at the top of Figure 3.20. Finally, the time difference between converted Sp and S waves can also be converted into the depth domain using a reference velocity model (e.g. IASP91).

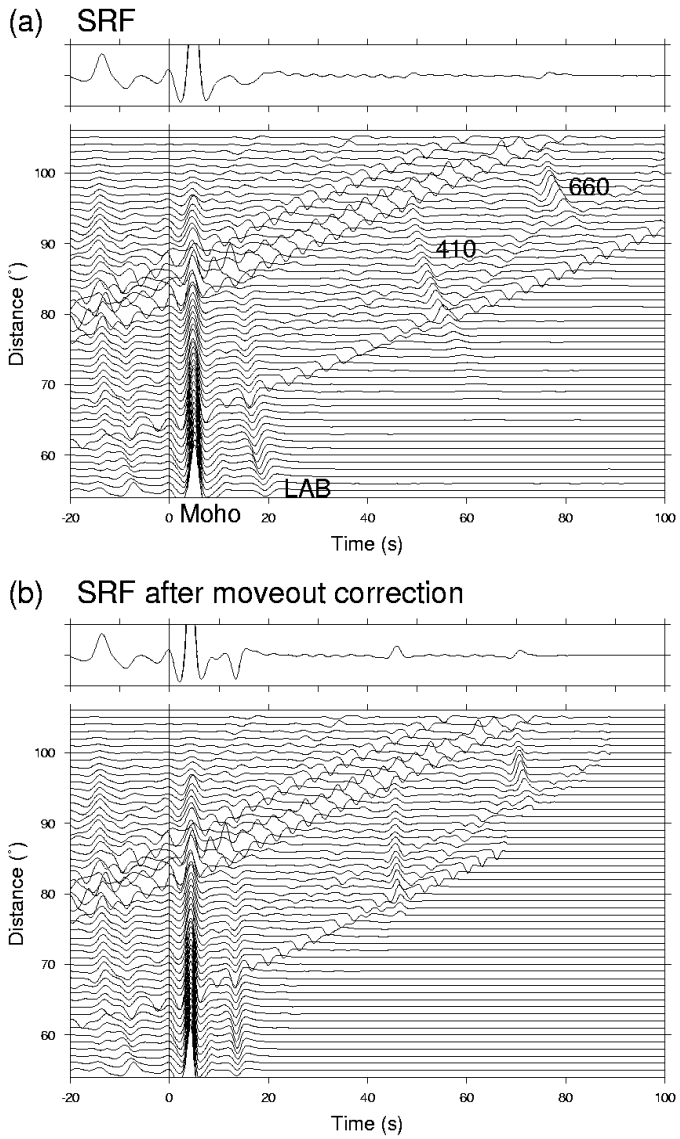

Fig. 3.20. Synthetic S receiver functions at a single station are computed using reflectivity method for a model containing a 35 km thick crust and 120 km thick lithosphere. The P velocity is considered to be 6.2 km/s in the crust, 8.0 km/s in the upper mantle with 5% reduction into the asthenosphere. Epicentral distances range between 60-110. a) By increasing epicentral distance, the delay times of Sp conversion decrease. b) Moveout corrections for Sp waves are applied to each sample. Reference slowness of 6.4 s/° is used. Sp converted phases are aligned vertically and their amplitudes are enhanced on the summation trace shown at the top.

The S receiver function as described before leads us to obtain the LAB with a resolution so far only known for the Moho.